EFFECTS OF GRAVITY WAVE DRAG IN THE MARTIAN ATMOSPHERE: SIMULATIONS WITH A GCM.

A. S. Medvedev, *Max Planck Institute for Solar System Research, Katlenburg-Lindau, Germany (medvedev@mps.mpg.de)*, **E. Yigit,** *University of Michigan, Ann Arbor, USA*, **P. Hartogh,** *Max Planck Institute for Solar System Research, Katlenburg-Lindau, Germany*.

Introduction:

Although observations show that gravity waves (GWs) are strong on Mars, little is known about their dynamical significance. Few observational estimates indicate that GW momentum deposition can reach from 1000 [*Fritts et al.*, 2006] to 4500 m s^{-1} sol^{-1} [*Heavens et al.*, 2010]. The previous GCM studies had several features in common: (1) upper boundaries of models were limited to ~80-100 km; (2) only terrain-generated harmonics with the observed phase velocity c=0 were considered; (3) they all utilized the Lindzen parameterization for calculating the drag produced by individual subgrid-scale harmonics. We quantify the GW momentum deposition due to waves of lower atmospheric origin by implementing our recently developed spectral nonlinear GW parameterization to the MAOAM GCM extended into lower thermosphere.

Gravity Wave Scheme:

The GW parameterization suitable for planetary thermospheres accounts for wave refraction by background wind and temperature, and for attenuation due to nonlinear effects (breaking and/or saturation) and dissipation (molecular diffusion and thermal conduction, ion friction, eddy diffusion). It treats the nonlinear interactions between the harmonics of the incidence spectrum, and converges to a well-known Hodges-Lindzen criterion of wave breaking for a single harmonic (but at $1/\sqrt{2}$ lower amplitudes) [*Medvedev and Klaassen*, 1995]. The scheme has been extensively tested with a terrestrial GCM extending from ~15 to 400 km [*Yigit et al.*, 2008; 2009*; Yigit and Medvedev*, 2009; 2010].

Estimates With MCD Data:

At first, the parameterization has been applied [*Medvedev et al.*, 2010] to the output wind and temperature from the Mars Climate Database (MCD). The appropriate molecular viscosity in the CO_2 gas atmosphere as a function of temperature and pressure has been used. Figure 1 presents the calculated GW momentum deposition for the zonal-mean wind and temperature averaged daily over the period L_s=270 to 300^0. It shows a huge (more than 10^5 m s^{-1} sol^{-1}) wave drag in the thermosphere. It obviously is not compatible with the given wind distribution. Once applied, it will modify the wind dramatically. Changing the launch height of the source, the amplitude of the harmonics and the shape of the spectrum do not alter this pattern significantly. The only reason for this enormous GW drag is the distribution of the background wind. These results indicate possible wind reversals in the lower thermosphere.

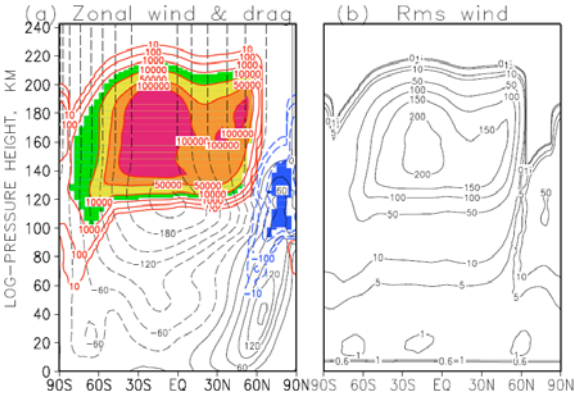

Figure 1. (a) The background zonal wind from MCD (contour lines) and the calculated GW drag in m s^{-1} sol^{-1} (shaded); (b) rms horizontal wind fluctuations due to GWs.

Model:

The MAOAM GCM used in our interactive calculations is essentially same as reported by *Hartogh et al.* [2005], but employs a spectral dynamical core. The GCM has the relevant physics parameterizations including a non-LTE radiation scheme for CO_2 heating and cooling. The upper boundary of the model has been extended to 10^{-5} Pa, or ~150 km., however without accounting for UV and EUV radiation. All calculations have been done at T21 spectral resolution (64 X 32 gridpoints in longitude and latitude) on 63 vertical levels.

Observational Constraints:

Observational constraints for GWs in the lower atmosphere include the MGS radio occultation data [*Creasey*, 2006]. They found that wave potential energy per unit mass, E_p, averaged between 10 and 30 km is typically up to few J kg^{-1} at mid- to high latitudes. In low latitudes, it increases up to 25 J kg^{-1}. For GWs with vertical wavelengths shorter than approximately a scale height, those we are most concerned with, E_p is about twice weaker. This corresponds to rms wind variations due to GWs, |u'|, up to 5-7 m s^{-1}. In the upper atmosphere, the ODY aerobraking data [*Fritts et al.*, 2006] give |u'| up to 70 m s^{-1} and wave momentum fluxes up to 2000 m^2 s^{-2} at ~100 km or somewhat higher. These quantities can be compared with the output of the GW parameterization

Results

A one-year GCM simulation for the fixed dust opacity τ=0.2 in visible has been performed with the interactive GW scheme. The waves were launched from *p*=250 Pa (or ~8 km), just above the layers frequently affected by atmospheric convection. The source spectrum included 30 harmonics with *c* from -60 to +60 m s^{-1} directed along the local wind. This setup produced the best results in numerous simulations for Earth. The shape of the spectrum with smaller amplitudes for faster waves was also chosen from the experience gained with terrestrial GCMs. Note that no sponge layer was used in the simulations, unlike in many other GCMs. Thus, there was no other artificial physics introduced at upper levels.

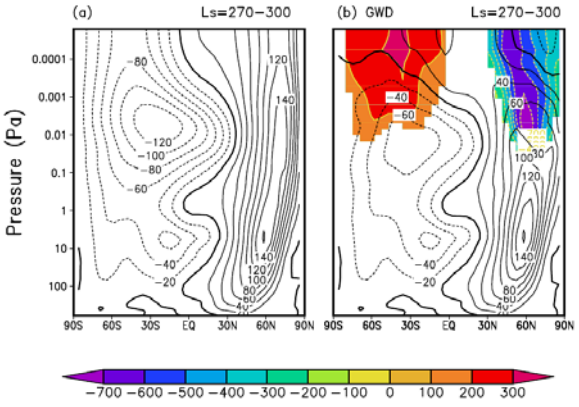

Figure 2. Zonal wind simulated (a) without and (b) with the GW parameterization (contours). Shaded is the GW drag (in m s^{-1} sol^{-1}).

Figure 2 compares the simulated zonal wind averaged over L_s=270 and 300^0 from the runs with and without GWs. The main result of inclusion of the GW drag scheme is the closure of both easterly and westerly jets, and a significant reduction of the easterlies in the summer (Southern) hemisphere. This pattern holds when the parameters of the source spectrum change. The main effect on the meridional wind (not shown here) is a weakening of the pole-to-pole transport in the summer hemisphere and its intensification in the winter one. The lower thermospheric temperature in the run with GWs is higher in both polar regions, especially over the winter pole, and lower in midlatitudes of the winter hemisphere.

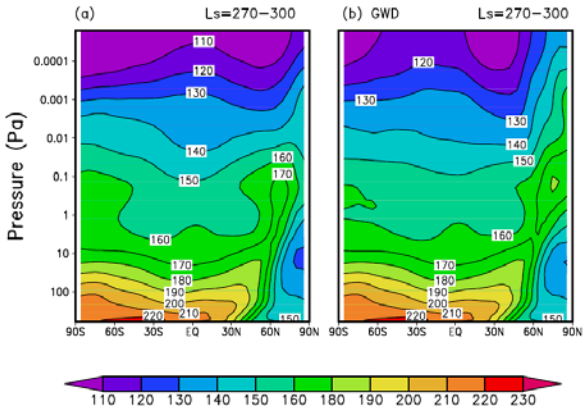

Figure 3. Zonal-mean temperature simulated (a) without and (b) with gravity wave scheme.

References

Creasey, J.E., Forbes, J.M., Hinson, D.P., 2006. Geophys. Res. Lett 33, L01803, doi:10.1029/2005 GL02 4037.

Fritts, D.C., Wang, L., Tolson, R.H., 2006. J. Geophys. Res. 111, A12304, doi:10.1029/2006 JA011897.

Hartogh, P. et al., 2005. J. Geophys. Res., 110, E11008, doi:10.1029/2005JE002498.

Heavens, N.G et al., 2010. Icarus, 208, 574--589, doi:10.1016/j.icarus.2010.03.023.

Medvedev, A.S., Klaassen, G.P., 1995. J. Geophys. Res. 100, 25841--25853.

Medvedev, A.S., Yigit, E., Hartogh, P., 2010. Icarus, doi:10.1016/j.icarus2010.10.013.

Yigit, E., Aylward, A.D., Medvedev, A.S., 2008. J. Geophys. Res 113, D19106, doi:10.1029/2008 JD010135.

Yigit, E., Medvedev, A.S., Aylward, A.D., Hartogh, P, Harris, M.J., 2009. 114, D07101, doi:10.1029/ 2008JD011132.

Yigit, E., Medvedev, A.S, 2009. Geophys. Res. Lett. 36, L15807, doi:10.1029/2009GL038507.